



Characterization and optical studies of pure and Sb doped ZnO nanoparticles

*Shashi B. Rana¹, Amarpal Singh², Satbir Singh¹

¹Assistant Professor, Dept. of ECE, G.N.D.U, Regional Campus, Gurdaspur, India

²Associate Professor, Dept. of ECE, B.C.E.T, Gurdaspur, Punjab, India

Received 13 Feb. 2012; Revised 10 May 2012; Accepted 22 May 2012

Abstract

In the present work, a direct precipitation method using wet chemical reaction was used to synthesize pure and Sb doped ZnO nanoparticles. The zinc nitrate and sodium hydroxide were used as starting materials or precursors to precipitate the desired pure ZnO nanoparticles followed by calcinations at 500°C. For the preparation of Sb doped nanoparticles stoichiometric amount of respective metal nitrate was dissolved in the zinc nitrate solution before precipitation. The phase purity and crystallite size of pure and Sb doped ZnO particles were characterized via X-ray diffraction and scanning electron microscopy. The X-ray diffraction results indicated that the synthesized ZnO powders had a pure single phase wurtzite structure. The average particle sizes of pure ZnO was found to be 32 nm and average particles size for Sb doped ZnO was found to be in the range of 19-28 nm according to XRD measurements. Incorporation of dopant Sb influenced the particle size of the ZnO nanoparticles. Photoluminescence spectra of commercial and Sb doped ZnO were plotted for different composition (1%, 3%, 5%) of doped Sb, showed that there was increase in intensity for Sb doped ZnO (1%, 3 % Sb) nanoparticles and decrease in intensity for 5 % Sb doping. Finally UV-Vis spectra of pure synthesized ZnO and Sb doped ZnO nanoparticles showed blue shift in wavelength with respect to bulk value due to quantum confinement effect.

Keywords: Sb Doped ZnO nanoparticles; Precipitation method; UV-Vis spectra; XRD; PL.

PACS: 71.35.-y ; 78.67.Bf ; 78.66.Hf ; 78.55.Et; 81.20.Ka; 81.07.Wx.

1. Introduction

Recently, there has been tremendous interest in group II-VI compound semiconductor ZnO because of its direct band-gap of 3.37 eV at room temperature with a large exciton binding energy of 60 MeV which have optoelectronic applications in the blue, violet and ultra-violet regions of the electromagnetic spectrum [1]. Semiconductor nanoparticles of ZnO have also received much attention as a potential candidate material for solar energy conversion, varistors, transparent UV protection films [2], chemical sensors [3], optical sensors etc. [4-7], due to their unusual electrical, optical, mechanical properties. These properties results from quantum confinement effects. Generally most ZnO

*) For correspondence, Tel :+(91)1874-22139, Fax: + (91)1874-242678, E-mail: shashi_rana12@yahoo.co.in

nanoparticles have generally n-type character, even in absence of intentional doping. Native defect such as oxygen vacancies or zinc interstitial are assumed to be origin of n-type character. The major obstacle for wide ranging applications in electronics and photonic devices rests with difficulty of p-type doping of ZnO nanoparticles. The quest for stable, p-type ZnO is challenging because the electronics and optical properties are sensitive to minute concentration of dopants and impurities. A possible clarification has been anticipated, based on theoretical calculations, that unintentional substitutional hydrogen impurities are responsible for n-type [8] character of ZnO nanoparticles. However controllable n-type doping is simply achieved by substituting Zn with group-III elements like Al, Ga, In or by substituting oxygen with group-VII elements like chlorine or iodine. On the other hand reliable p-type doping of ZnO remains difficult to achieve. The major obstacle of ZnO for broad ranging application in electronics and photonics rests with difficulty of p-type doping. The quest for stable p-type ZnO is challenging, because the electronics and optical properties of ZnO are very susceptible to minute concentration of dopants, impurities, and minute perturbation of the lattice. A range of acceptors and doping technique have been tested and investigated to achieve p-type conductivity. The role of crystal defects in ZnO is a subject of significant interest because the understanding of good p-type conductivity will need an understanding of various interactions between acceptors and crystal defects, either native or doping-induced. Known p-type dopants include group-I elements like Li, Na, K; group-V elements like N, P, As, Cu and Ag [9-11]. Many time ionic radii of these elements and size mismatches with host elements. However, the majority of dopants are soluble [12-13] and it may form deep acceptors and produce insignificant p-type conduction at room temperature. Nitrogen has been regarded as most appropriate impurity for p-type doping in ZnO. However nitrogen is deep level acceptor & hence cannot produce hole conductivity [14] in ZnO. On the other hand if dopant is shallow, the free carrier it produces may be compensated by oppositely charged defects. Hence main challenges behind p-type doping of ZnO: Issue of low doping solubility, deep level formation and acceptor ionization need to be addressed. Successful p-type doping for ZnO nanostructure will significantly enhances their future applications in nanoscale optoelectronics devices. However, for the present work we have planned to synthesis nanocrystalline ZnO (Undoped & doped) by chemical route. In this study, an attempt to synthesize Sb-doped ZnO was made for improving its optoelectronics properties. In order to better understand these properties of Sb doped nanoparticles, the choice of sample preparation method therefore is of greatest importance. The preparation method should be the one that can compel the doped Sb ions into substitutional site and have atomic scale homogeneous mixing with host atoms without the formation of secondary phases. For the same reason, extensive research efforts have been carried out worldwide to synthesize nano-sized undoped and doped particles using various methods [15-20] such as thermal decomposition, chemical vapor deposition, sol-gel, spray pyrolysis, microemulsions and precipitation. The precipitation method compared with other traditional methods provides a simple growth process for large-scale production, and which of course is an efficient and inexpensive way. The distinctive feature of this process is that an atomic scale homogeneous distribution of doped Sb ions in the host matrix can be achieved. The aim of the present study is to synthesize phase pure nanoparticles of pure and Sb doped ZnO via direct precipitation method followed by structural characterization using X-ray diffraction (XRD), Energy dispersive x-ray spectroscopy (EDS), scanning electron microscopy (SEM) and optical properties are characterized by UV-Vis spectroscopy and photoluminescence spectroscopy. A UV-Vis spectrum shows that band gap energy increase with different concentration (1%, 3% and 5% Sb) in host ZnO nanoparticles. Finally photoluminescence spectra of pure and doped ZnO showed that there was increase in PL intensity of Sb doped nanoparticle for 1 % and 3 % Sb doped ZnO for both in UV and in the

visible region of spectrum and decrease in PL intensity for 5 % Sb doping for both the region of PL spectra.

2. Experimental Details

Here direct precipitation method is used to synthesize the nanoparticles of pure and Sb doped ZnO nanoparticles. Zinc nitrate ($\text{Zn}(\text{NO}_3)_2$) and sodium hydroxide (NaOH) were used as precursors of the ZnO particles. The aqueous solution of metal nitrates was prepared from pure metal by dissolving in concentrated nitric acid. A known quantity of NaOH was dissolved in deionised water and the resulting solution was mixed with the zinc nitrate solution leading to the formation of white precipitates. The precipitates were washed several times with deionised water and finally with ethyl alcohol to remove the impurities. The resulting fine powder was dried in an oven at 100°C for 15h. The as dried powder was grounded and then calcined at temperatures 500°C for 4h. For present study, we prepared pure ZnO, and doped Sb for which the stoichiometric amount of respective metal nitrate was dissolved in the zinc nitrate solution before precipitation. Phase purity of the nanopowder samples was examined by (XRD) using Cu $K\alpha$ radiation, 40kV and 30mA, time constant of 0.5s and crystal graphite monochromator. With increasing annealing temperature, the typical tendency of increasing intensity of all the peaks in XRD pattern was observed. From XRD line broadening, the average particle sizes for nanocrystalline powders were deduced using Scherrer's equation ($D = 0.9\lambda / \beta \cos\theta$), where D is the crystallite diameter, λ is the radiation where D is the crystallite diameter; λ is the radiation wavelength and θ the incidence angle. The value of β was determined from the experimental integral peak width. Values were corrected for instrumental broadening. The composition studies were done by Energy dispersive X-ray spectroscopy (JEOL JSM 6360LA, Japan). The morphologies and size of ZnO nanoparticles were obtained by TEM (JEOL JEM 1230, Japan). The optical absorption measurements were done with a double beam spectrophotometer (UV-Vis, Spectrophotometer, special double 8 auto cell). While FTIR spectrum of prepared ZnO and Sb doped ZnO were measured by Shimadzu FTIR-8400S over the wavelength range of $400\text{-}4000\text{ cm}^{-1}$. The photoluminescence spectra was measured at room temperature with an accent PL mapping system (2000 rpm). The sample was excited with 325 nm line of He-Cd laser. The luminescence was dispersed and recorded with a CCD.

3. Results and Discussion

3.1 X-Ray Diffraction (XRD)

Figure 1 reports the typical XRD spectra of prepared undoped (pure) and Sb-doped ZnO powders with different composition of Sb. For comparison purpose we have included samples of commercially prepared ZnO nanoparticles also in our discussion. All diffraction peaks were indexed to hexagonal wurtzite ZnO. Figure 1 (a) & (b) reveals that highly crystalline wurtzite structures with no peaks corresponding to Sb for commercial and pure ZnO prepared at 500 degree centigrade. Diffraction peaks related to the impurities were not observed in the XRD pattern, confirming the high purity of the commercial and synthesized powder. Three pronounced ZnO diffraction peaks (100), (002) and (101) appear at $2\theta = 31.72^\circ$, 34.38° and 36.22° , respectively. When Sb-doping begins, very small peak diffraction appeared at 28.8° Fig. 1(b) which is increased in intensity with increasing Sb doping ratio Fig.1(c), 1(d) and 1(e) [21]. The full width of (002) peak at half maximum became narrower in all peaks. The average crystallite size of ZnO particles and Sb-doped

ZnO particles was deduced from Scherrer's equation [22]. The average crystallite size of ZnO was in the range of 19-28 nm. On doping diffraction peaks were getting narrower, which signifies that on doping particles size decreases. The enhanced intensities of the XRD peaks of doped ZnO nanoparticles suggest better crystallinity. Hence on increasing doping concentration ZnO crystallites size decreases. The reduction of the particle size was observed from XRD measurements for doped ZnO nanoparticles with incorporation of Sb dopant. This may be explained by decrease of sintering rate due to incorporation of Sb dopant atoms into the ZnO lattice. Average crystallite size of ZnO and doped ZnO with different composition of Sb was calculated from Debye Scherrer's formula $D = 0.9\lambda / B_{2\theta} \cos \theta$ where λ is wavelength of X-ray used which is taken as 1.5406 \AA , D is average crystallite in nm and $B_{2\theta}$ is angular width in radians.

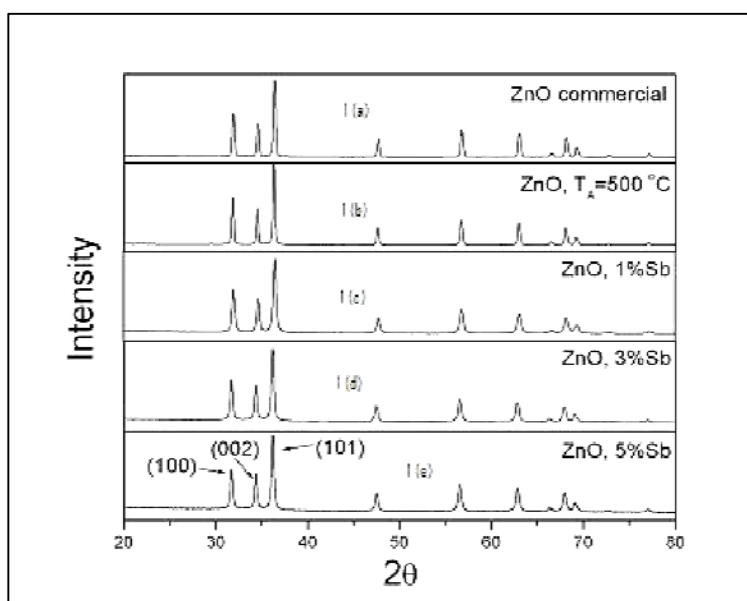


Figure 1: XRD spectra of (a) commercial (b) Pure ZnO (at T_A 500°C) (c) ZnO, 1% Sb, (d) ZnO, 3% Sb (e) ZnO, 5% Sb.

3.2 SEM and EDS

The morphology of nanocrystalline pure ZnO and doped ZnO nanopowders was revealed by SEM. Figure (2) reports the SEM image of pure and ZnO doped with different composition of Sb as 1 % Sb, 3% Sb and 5% Sb respectively. Figure 2 (D) clearly indicates that the synthesized pure ZnO nanoparticles are well defined and distinguishable from each other. At 1 % composition of Sb dopant in ZnO nanoparticles the particle size become smaller and darker and homogenous morphology is obtained. These SEM image reveals that the surface morphologies of ZnO nanoparticles are affected by concentration of doped Sb. Almost same homogenous structure will be obtained for doping of ZnO with 3% Sb. But when ZnO doping is increased from 3% to 5% Sb then finer particles were observed with distinguishable separate dark and lighter areas or heterogeneous morphology, indicating excess Sb.

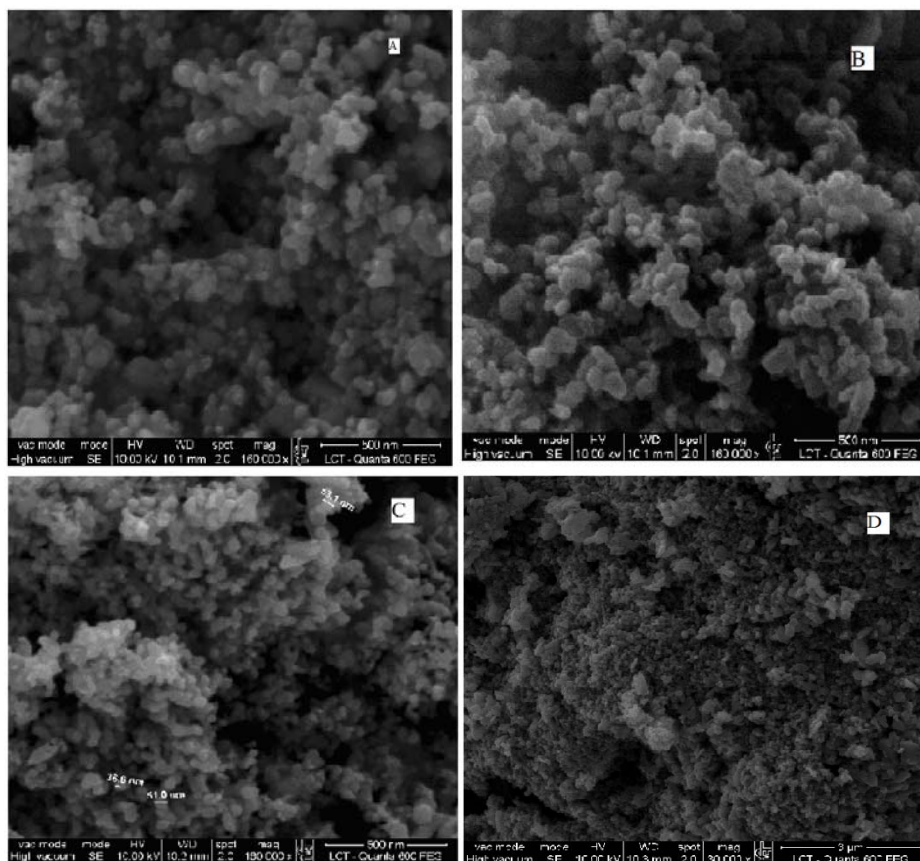
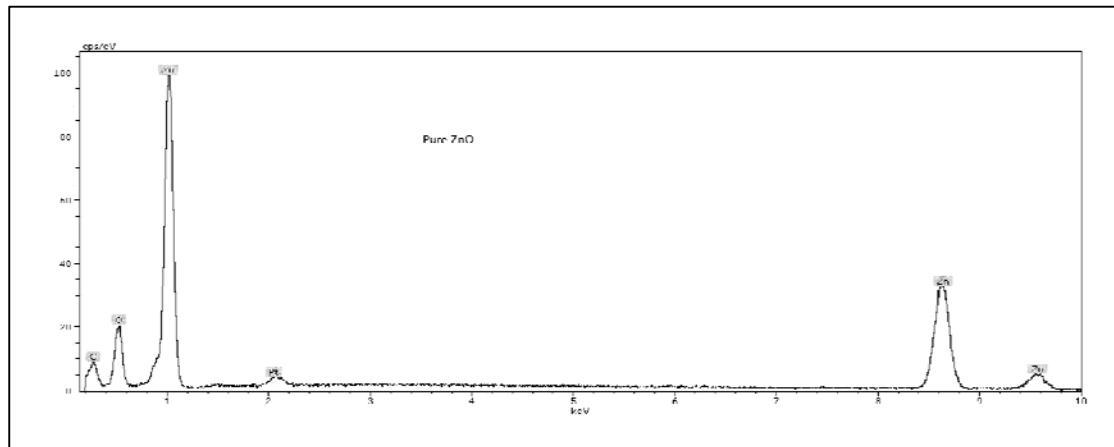
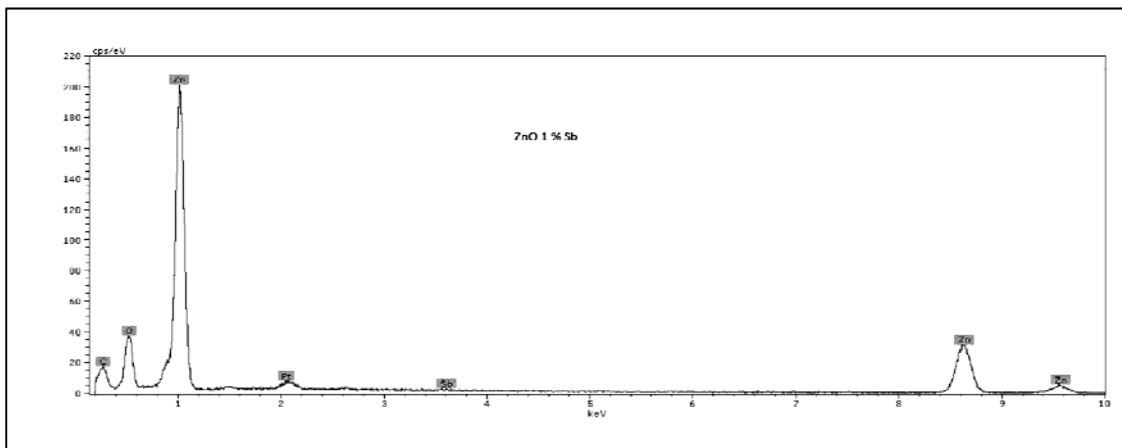


Figure 2: SEM Image of (A) ZnO doped with 1% Sb (B) ZnO doped with 3% Sb (C) ZnO doped with 5 % Sb (D) Pure ZnO.

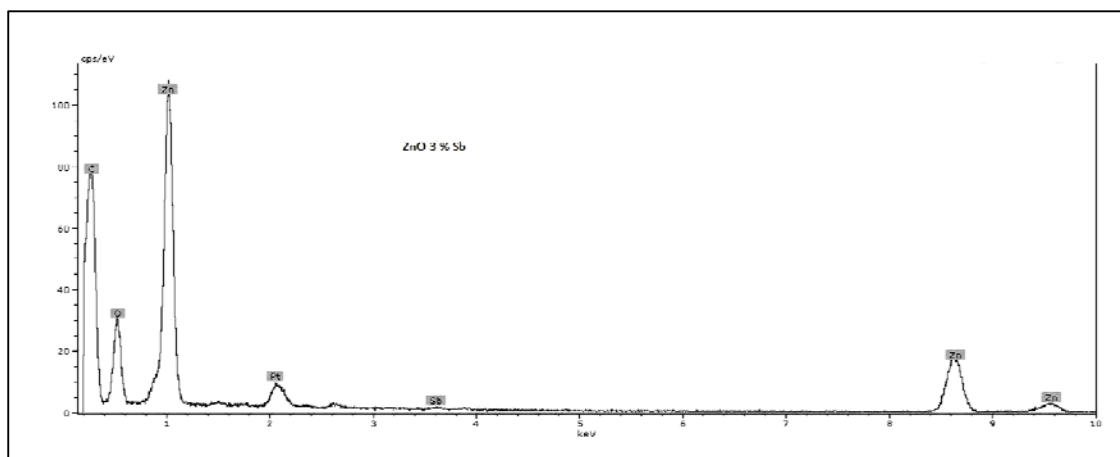
In SEM, the grain size was measured by the difference between the visible grain boundaries whereas in XRD, the measurement was extended to the crystalline region that diffracted X-rays coherently. Therefore, the XRD measurements led to smaller size. While Figure 3 reports the EDS spectra of pure synthesized ZnO and for ZnO nanoparticles doped with different composition (1% to 5%) of Sb with no other impurities were detected. The EDS results as shown in Figure 3 indicate that no other element but Zn and O were present in pure ZnO samples whereas Zn, dopants Sb and O were present in doped samples. The small Pt peak appearing in the spectra is due to the coating of the sample. The peak of Sb incorporated in EDS spectra will go on increasing as we increased concentration of doped Sb (1 % to 5 %) as shown in Figure 3 (b) to figure 3(d).



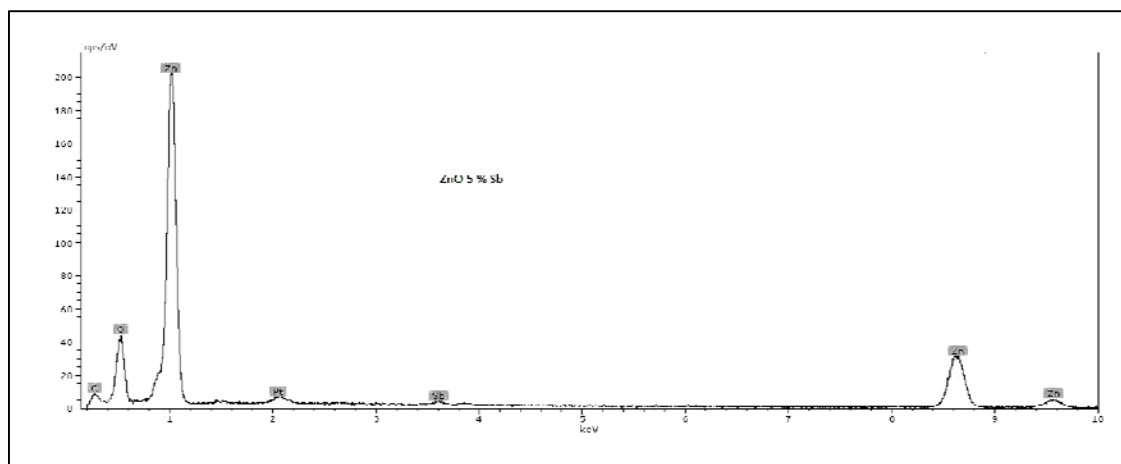
(a)



(b)



(c)

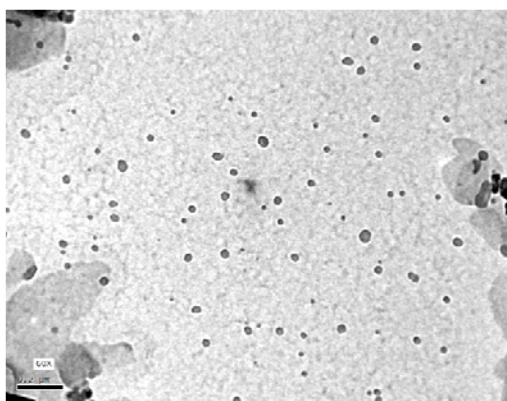


(d)

Figure 3: EDS spectra for pure and Sb-doped ZnO particles (a) Pure ZnO (b) ZnO doped with 1% Sb (c) ZnO doped with 3% Sb and (d) ZnO doped with 5% Sb.

3.3 TEM Spectrum Analysis

The crystal size and morphology of pure ZnO, and ZnO doped with 1% to 5% Sb were investigated by TEM measurements as shown in Figure 4. The particle size of pure ZnO nanoparticles was in the range of 20–30 nm shown in Figure 4 (a). However, the doped ZnO samples have hexagonal particles in the range of 10–20 nm shown in Figures 4(b), 4(c) and 4 (d) when Sb doping composition has been increased from 1% to 5%. It is evident that on doping process we get reduced particle size of the ZnO particles. These results were compatible with their counterparts of XRD measurements also. Furthermore, by comparing the three TEM figures, it is clear that the presence of dark spots of Sb were increased as percentage (%) doping of Sb is increased. In Figure 4 (a) there were no dark spots noticed for pure ZnO which giving rise to homogeneous composition.



(a)

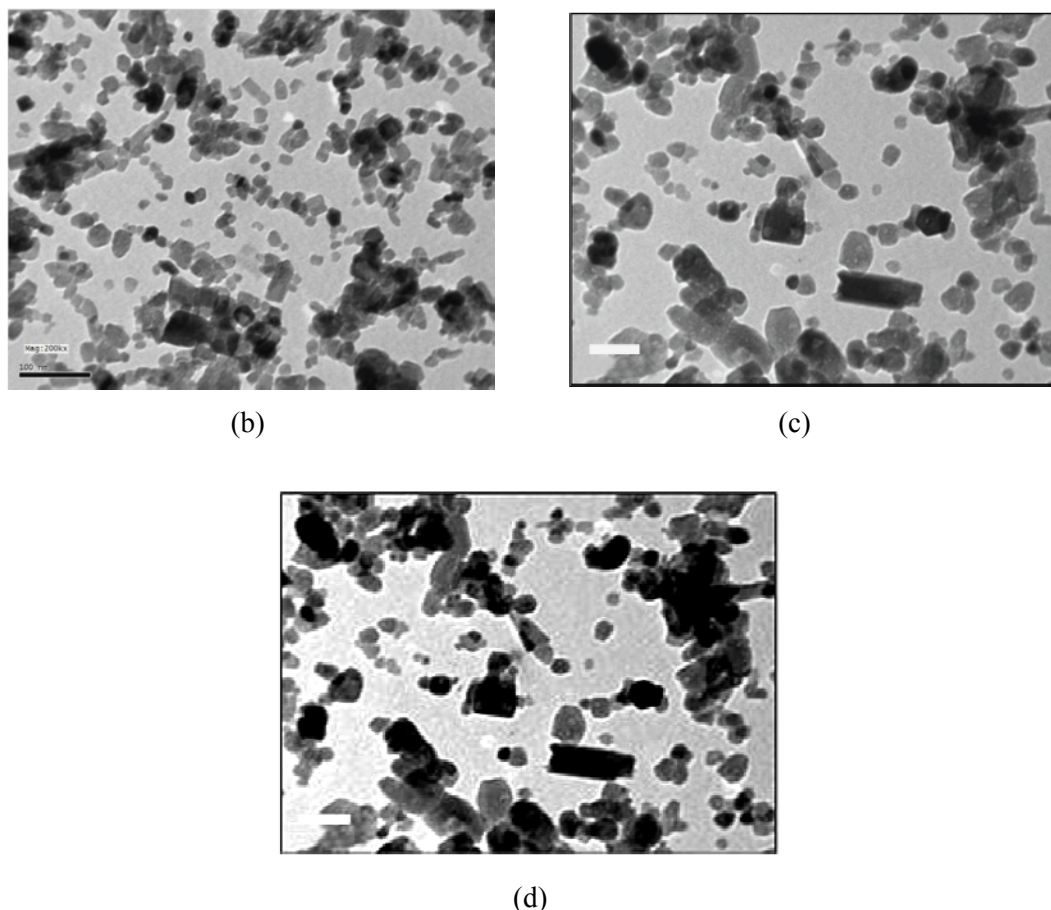


Figure 4: TEM Image of (a) Pure ZnO (b) ZnO doped with 1% Sb, (c) ZnO doped with 3% Sb (d) ZnO doped with 5 % Sb.

3.4 Fourier Transform Infrared Spectrophotometry (FT-IR)

Figure 5 shows the FT-IR spectrum of the ZnO and ZnO doped with 1% to 5% Sb. The broadband at 3400 cm^{-1} is assigned for asymmetric and symmetric stretching of vibrational -OH groups. However, the band at 1600 cm^{-1} is assigned for the H-O-H bending vibration. The IR absorption band at 440 cm^{-1} originates from the Zn-O stretching vibration. Regarding the FT-IR of the Sb doped samples, a new peak at 688 cm^{-1} is indicated, which is absent in the spectrum of pure ZnO. This new peak at 688 cm^{-1} is due to the presence of Sb_2O_3 [23] with increasing order in its intensity from different composition of doped Sb (1% to 5%) with ZnO nanoparticles as shown in Figure 5.

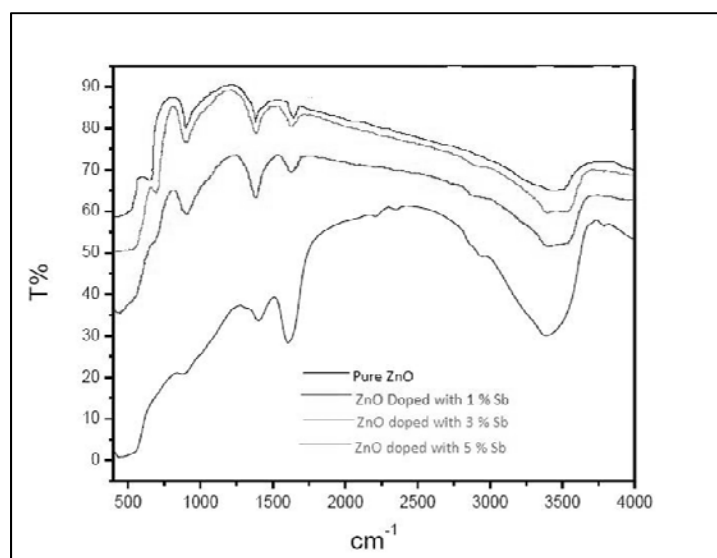


Figure 5: FTIR spectra of (a) Pure ZnO, (b) ZnO, 1% Sb (C) ZnO, 3% Sb.

3.5 UV-Vis Absorption Spectroscopy

Optical properties of ZnO particles become important as the size of particles is reduced to nanoscale. Figure (6) shows the UV-Visible absorption spectra of pure and Sb doped ZnO at different percentage (%) composition of the Sb. The absorption coefficients (α) were calculated and plotted for the direct transition $(\alpha h\nu)^2$ versus $h\nu$ of the undoped ZnO and ZnO:Sb i.e. doped Sb at different composition (1 % Sb, 3 % Sb and 5 % Sb). The value of the band gap energy (E_g) of undoped nanocrystalline ZnO nanoparticle was 3.26 eV and increased by incorporation of Sb doping, as it was 3.309 eV for doping 1%Sb, 3.318 eV for 3%Sb, and 3.329 eV for 5% Sb. This enhancement in band gap is due to the Sb incorporation and the high carrier concentration that moved the optical absorption edge towards lower energy and broadened the energy gap [24]. The dopant may dominantly contribute to the width of localized states within the optical band of ZnO. Introduction of the dopant Sb into ZnO thus increases the width of the localized states and hence results in increase the the band gap energy. The band gap energy (E_g) of sample is determined by the formula $\alpha h\nu = E_d (h\nu - E_g)^{1/2}$ where α is absorption coefficient, $h\nu$ is energy of photon, E_g is direct band gap and E_d is constant [25]. By plotting $(\alpha h\nu)^2$ as a function of photon energy, and extrapolating the linear region of curve to absorption equal to zero as shown in Figure 6 gives the value of direct band gap (E_g). Unique exciton absorption at 377 nm is observed in the absorption spectrum at room temperature, which is blue shifted with respect to bulk absorption edge value appearing at 380 nm. It is apparent that absorption edge shifts to higher energy or lower wavelength with decreasing the size of ZnO nanoparticles i.e. particle size start decreasing due to percentage (%) increase in doping. This marked shift in absorption edge is due to quantum confinement effect. It is clear from the figure that absorption edge start shifting to lower wavelength or higher band gap energy as Sb doping varied from 1 % to 5 %. Blue shift in absorption spectra will be due to increase in band gap energy with decrease in particle size results due to quantum confinement effect as doping concentration of dopant Sb varied (1 % to 5 %) in ZnO nanoparticles. Wide region of the peaks indicates the size distribution or smaller size of ZnO nanoparticles with the variation in doping level, as evident by XRD results.

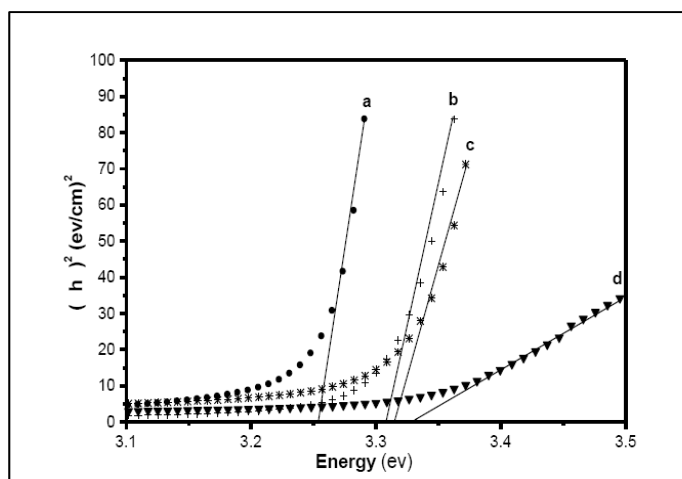


Figure 6: Band gap using UV-Vis spectra of (a) Pure ZnO (b) ZnO, 1% Sb (c) ZnO, 3% Sb (d) ZnO, 5% Sb.

3.6 Photoluminescence Spectra Study

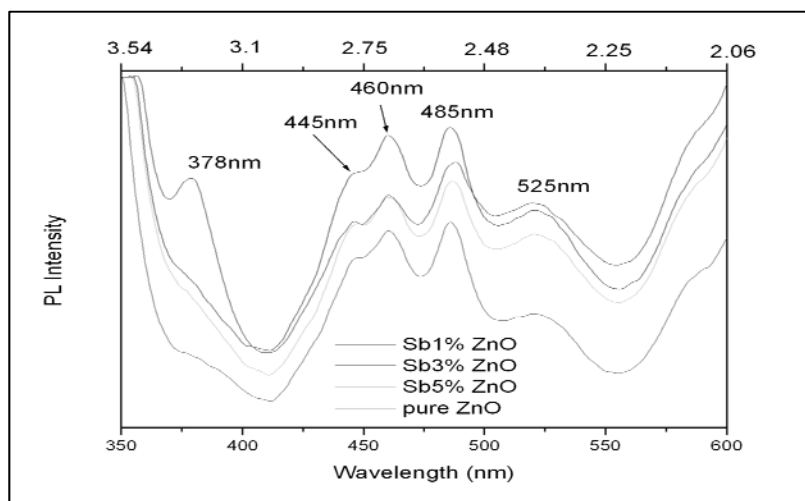


Figure 7: PL Spectra of Pure ZnO, ZnO doped with 1% Sb, ZnO doped with 3% Sb and ZnO doped with 5% Sb.

Figure 7 shows the room temperature photoluminescence spectra of the pure ZnO sample and ZnO nanoparticles sample doped with different composition of Sb (1% Sb, 3% Sb, and 5% Sb) measured using a Xenon laser at 325 nm as an excitation source. For comparison purpose, measurement was carried out on pure synthesized ZnO nanoparticles sample synthesized at 400°C with average particle size of 32 nm as confirmed by XRD spectra also. Figure 7 reports PL spectra of purely synthesized ZnO nanoparticles consisting of five significant emission peaks at 378 nm (3.28 eV), a blue band-I at 445 nm (2.79 eV), a blue band-II at 460 nm (2.70 eV), a blue-green band at 485 nm (2.56 eV) and a weak band at 525 nm (2.36 eV). The strong UV emission corresponds to exciton recombination related near band edge emission of ZnO [26-27]. The blue and bluish green emissions are believed to be due to presence of various surface defects in ZnO [28]. The green band emission corresponds to the singly ionized oxygen vacancy in ZnO, and this emission is due to recombination of a photo-generated hole with the single ionized charge state of the particular defect [29]. The less intensity of the green emission may be due to less density of

the oxygen vacancies during the synthesis of ZnO. Strong intensity of the UV emission should be attributed due to the high purity and perfect crystalline nature of pure synthesized ZnO nanoparticles. In all the doped sample UV emission is not present which imply that on doping size of ZnO nanoparticles goes on reducing. Photoluminescence spectra as in Figure 7 reports that in case of doped Sb the PL emission band around 525 nm (2.36 eV) has been observed and attributed to the oxygen vacancies in ZnO nanoparticles. The high intensity of 445 nm peak in the 1% Sb sample reveals that a large amount of interstitial Zn might be present in the doped ZnO sample. Continuous increase of Sb concentration up to 3% helps reduce both Zn interstitial and oxygen vacancies in the doped ZnO sample. This trend suggests that the introduction of Sb is expected to passivate the Zn interstitials and oxygen vacancies, leading to the reduction of these defects. Too high concentration of Sb up to 5%, however, drastically reduces the relative intensity of the band-edge emission at 378 nm. This study shows that the crystallinity becomes worse at high concentration of Sb doping, which is not unfair. The p-type ZnO materials doped with Sb have been reported by numerous research groups [30-32]. SbZn is likely formed in the Sb doped samples, even though isolated SbZn acts as a donor and results in n-type conductivity. But, Limpijumnonng et al. [33] pointed out that the SbZn-2VZn complex was assumed to be the most expected contender to form a shallow acceptor level in large-sized mismatched group-V-doped ZnO samples. The n-type conductivity reported in 1% Sb-doped ZnO sample in our present work indicates that this low concentration of dopant is inadequate to convert the conductivity from n- to p-type. Even though SbZn might be formed in the doped ZnO samples, they could still be isolated or SbZn-2VZn concentration is still too much low to exhibit p-type conductivity. This hypothesis is consistent with our PL measurements. The reduced intensity of Zn interstitial for the highly doped (5 % Sb) ZnO samples suggests that the amount of Zn interstitial could be considerably reduced and the possibility of forming SbZn-2VZn complexes is enhanced or increased. Once the concentration of SbZn-2VZn complexes is high enough, the conductivity would change from n- to p-type.

4. Conclusion

Precipitation method has been successfully used for synthesis of pure and doped ZnO nanoparticles with different percentage (%) composition of Sb. The structural and morphology of synthesized pure and Sb doped ZnO nanoparticles have been confirmed by XRD, SEM, and TEM measurements. XRD measurements showed that pure synthesized ZnO nanoparticles samples exhibits hexagonal wurtzite structure with size of 32 nm, while doped ZnO nanoparticles showed particle size variation in the range of 19 nm to 28 nm with varied percentage (%) composition of Sb. The dopant Sb has significant influence on morphology of doped ZnO nanoparticles as confirmed by SEM measurements. Optoelectronic investigation has been carried out by employing photoluminescence and UV-Visible spectroscopy. Photoluminescence spectra results have shown and confirmed that for pure ZnO nanoparticles samples exhibits UV emission peak at 378 nm in UV region accompanied by different peaks in the visible region. But with the increase in doping (%) composition of Sb i.e. from 1 % to 3 % we obtained corresponding increase in PL intensity in both UV and in visible region of spectra. But this intensity goes on decreasing for 5 % Sb doping. UV-visible absorption spectra results of Sb doped ZnO nanoparticles indicates that there is blue shift in absorption spectra on varying Sb doping concentration. Blue shifted absorption edge or large value of band gap energy with respect to bulk value (380 nm) has confirmed that pure and doped synthesized ZnO nanoparticles exhibit quantum confinement effect.

References

- [1] Anderson Janotti and Chris G Van de Walle, *Rep. Prog. Phys.*, **72** (2009) 126501
- [2] C. H. Lu and C. H. Yeh, *Mater. Lett.*, **33** (1997) 129
- [3] C. H. Lu and C.H. Yeh, *Ceram. Int.*, **26** (2000) 351
- [4] E. Ziegler, A. Heinrich, H. Oppermann and G. Stover, *Phys. Status Solidi*, **A 66** (1981) 635
- [5] F. C. Zhang, Z. Y. Zhang, W. H. Zhang, J. F. Yan, and J. N. Yun, *Chinese Physics Letters*, **25**(10), (2008) 3735
- [6] F. X. Xiu, Z. Yang, L. J. Mandalapu, D. T. Zhao, J. L. Liu and W. P. Beyermann, *Appl. Phys. Lett.*, **87** (2005) 152101
- [7] G. A. Hirata, J. Mckittrik, T. Cheeks, J. M. Siqueiros, J. A. Diaz, O. Contreras and O. A. Lopez, *Thin Solid Films*, **288** (1996) 29
- [8] J. L. Lyons, A. Janotti and C. G. Van de Walla, *Applied Physics Letter*, **95** (2009) 252105
- [9] J. Wang and L. Gao, *Inor. Chem. Com.*, **6** (2003) 877
- [10] J. Wang and L. Gao, *Solid State Commun.*, **132** (2004) 269
- [11] K. Vanheusden, W. L. Warren, C. H. Sesger, D. R. Tallant, J. A. Voigt and B. E. Gnage, *J. Appl. Phys.*, **79** (1996) 7983
- [12] K. T. R. Reddy and R. W. Miles, *J. Mater. Sci. Lett.*, **17** (1998) 279
- [13] L. J. Mandalapu, F. X. Xiu, Z. Yang and J. L. Liu, *J. Appl. Phys.*, **102** (2007) 023716.
- [14] M. Andres-Verges and M. Martinerez-Gallego, *J. Mater. Sci.*, **27** (1992) 3756
- [15] M. Aslam, V. A. Chaudhary, I. S. Mulla, S. R. Sainkar, A. B. Mandale, A. A. Belhekar and K. Vijayamohanan, *Sens. Actuators A-phys.*, **75** (1999) 162
- [16] M. C. Carotta, A. Cervi, V. di Natale et al., *Sensors and Actuators B*, **137**(1), (2009) 164
- [17] N. K. Zayer, R. Greef, K. Roger, A. J. C. Grellier and C. N. Pannell, *Thin Solid Film* **352** (1999) 179
- [18] O. Kluth, B. Rech, L. Houben, S. Wieder, G. Schope, C. Beneking, H. Wagner, A. Loffl and H. W. Schock, *Thin Solid Films*, **351** (1999) 247
- [19] P. Nunes, B. Fernandes, E. Fortunan, P. Vilarinlo and R. Martins, *Thin Solid Films*, **337** (1999) 176
- [20] Q. Zhong and E. Matijević, *Journal of Materials Chemistry*, **6**(3), (1996) 443
- [21] R. Slama, F. Ghribi, A. Houas, C. Barthou, L. El. Mir, *Int. J. Nanoelectronics and Materials* **3** (2010) 133
- [22] S. J. Pearton, C. R. Abernathy, D. P. Norton, A. F. Hebard, Y. D. Park, L. A. Boatner, J. D. Budai, *Mater. Sci. Eng.* **R 40** (2003) 137
- [23] S. Limpijumnong, S. B. Zhang, S. H. Wei and C. H. Park, *Phys. Rev. Lett.*, **92** (2004) 155504
- [24] S. C. Lyu, Y. Zhang, H. Ruh, H. Lee, H. Shim, E. Suh and C. J. Lee, *Chem. Phys. Lett.*, **363** (2002) 134
- [25] T. J. Hsueh and C. L. Hsu, *Sensors and Actuators B*, **131**(2), (2008) 572
- [26] Ü. Özgüür, Ya. I. Alivov, C. Liu, A. Teke, M. A. Reshchikov, S. Doğan, V. Avrutin, S. -J. Cho and H. Morkoç, *J. Appl. Phys.*, **98** (2005) 041301

- [27] Uda Hasim, Elley Nadia, Shahrir Salleh, Int J. Nanoelectronics & Material, **2**(1), (2009) 119
- [28] X. Pan, Z. Ye, J. Li, X. Gu, Y. Zeng, H. He, L. Zhu, Y. Che, Appl. Surf. Sci. 253 (2007) 5067.
- [29] X. Y. Kang, T. D. Wang, Y. Han, M. D. Tao, Mater. Res. Bull. **32**, 1165 (1997),.
- [30] X. Y. Zhao, B. C. Zheng, C. Z. Li, H. C. Gu, Powder Techonl. **100**, 20 (1998).
- [31] Y. Li, G.S. Cheng, L.D. Zhang, J. Mater. Res. **15**, 2305 (2000).
- [32] Z.C. Jin, I. Hamberg, C.G. Granqvist, J. Appl. Phys. **64** (1988) 5117.
- [33] Z.Y. Ning, S.H. Cheng, S.B. Ge, Y. Chao, Z.Q. Gang, Y.X. Zhang, Z.G. Liu, Thin Solid Films **307** (1997) 50.